Pure Appl. Chem., Vol. 77, No. 1, pp. 327–338, 2005.
DOI: 10.1351/pac200577010327

Forced intercalation as a tool in gene diagnostics and in studying DNA–protein interactions*

Olaf Köhler[1], Dilip V. Jarikote[1], Ishwar Singh[1,2], Virinder S. Parmar[2], Elmar Weinhold[3], and Oliver Seitz[1,‡]

[1]Institut für Chemie der Humboldt-Universität zu Berlin, Brook-Taylor-Strasse 2, D-12489 Berlin, Germany; [2]Bioorganic Laboratory, Department of Chemistry, University of Delhi, Delhi 110 007, India; [3]Institut für Organische Chemie der RWTH Aachen, Prof.-Pirlet-Strasse 1, D-52056 Aachen, Germany

Abstract: Aromatic and heteroaromatic groups that are forced to intercalate at specific positions in DNA are versatile probes of DNA–DNA and DNA–protein recognition. Fluorescent nucleobases are of value since they are able to report on localized alterations of DNA duplex structure. However, the fluorescence of the vast majority of base surrogates becomes quenched upon intercalation in DNA. Peptide nucleic acid (PNA)-based probes are presented in which the intercalator dye thiazole orange (TO) serves as a fluorescent base surrogate. In these probes, fluorescence increases (5–60-fold) upon hybridization. PNA-bearing TO as fluorescent base surrogate could hence prove useful in real-time polymerase chain reaction (PCR) applications and in live cell analysis. Forced intercalation of aromatic polycycles can help to explore the binding mechanism of DNA-modifying enzymes. We discuss studies of DNA-methyltransferases (MTases) which commence methylation of nucleobases in DNA by flipping the target nucleotide completely out of the helix. A method for probing the base-flipping mechanism is suggested. It draws upon the observation that large hydrophobic base surrogates in the face of the swung-out base can enhance the DNA-enzyme binding affinity possibly by disrupting target base-stacking and stabilizing the apparent abasic site.

INTRODUCTION

Base-modified oligonucleotides have become increasingly popular as probes of DNA–DNA and DNA–protein recognition [1]. Fluorescent nucleobases such as 2-aminopurine [2] and many others [3] are invaluable tools owing to their ability to sense localized structural alterations, which is difficult to achieve by employing spacer-linked fluorophores. Recently, functional properties of DNA have been significantly expanded by replacing entire nucleobases with aromatic polycycles such as coumarin [4], pyrene [5], and others. In the following, we describe our efforts in two distinct research programs which both make use of base surrogates forced to intercalate at a chosen site.

*Paper based on a presentation at the 24th International Symposium on the Chemistry of Natural Products and the 4th International Congress on Biodiversity, held jointly in Delhi, India, 26–31 January 2004. Other presentations are published in this issue, pp. 1–344.

‡Corresponding author: Tel.: 49 30 20937446, Fax: 49 30 2093-7266; E-mail: oliver.seitz@chemie.hu-berlin.de

FORCED INTERCALATION AS A TOOL IN GENE DIAGNOSTICS

Genetic disorders present a threat to human health. There are various diseases such as Tay Sachs disease, Huntington's disease, Alzheimer's disease, cystic fibrosis, familial hypercholesterolemia, and even cancer that can be caused by gene mutations [6]. Molecular diagnostics opens the possibility to detect a developing disease before symptoms begin to appear, which is of particular importance in early cancer diagnostics. Gene-targeted assays are increasingly used and play an important role in various clinical settings. In analogy to protein-ligand binding assays, a specific probe molecule is designed to bind to the analyte or its binding partner. The design of specific binders for nucleic acid-based analytes is straightforward by employing oligonucleotide probe molecules, which bind to complementary nucleic acid targets with high affinity and selectivity in accordance to the Watson–Crick base-pairing rules. There are two distinct assay formats, in which DNA detection is achieved. In heterogeneous assays, either the analyte or the probe molecule is immobilized on a solid- or gel-phase, which facilitates the removal of unbound binding partners (Fig. 1a). Areas in which binding had occurred are detectable by means of a reporter group that is usually appended to the soluble binder. In contrast, homogeneous assays are comprised of only a solution phase, and separation of unbound from bound molecules is not possible (Fig. 1b). The design of a homogenous assay is conceptually more demanding. The probe molecules have to be equipped with dedicated reporter groups in which hybridization results in the alteration of a detectable variable. Albeit presenting significant challenges as far as the probe design is concerned, homogeneous DNA-detection methods offer the reward of allowing real-time measurements during the polymerase chain reaction (PCR) process itself (real-time PCR, QPCR) and even within live cells. Furthermore, single closed-tube assays are feasible, which reduces the contamination risk and speeds up analysis.

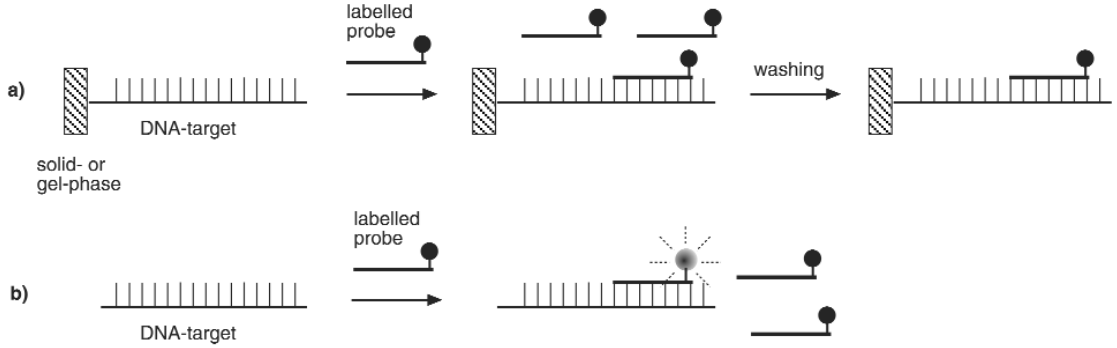

Fig. 1 Heterogeneous vs. homogenous DNA detection.

Most assays rely on the use of labeled probe molecules and the distance-dependent interactions between the two labels. For example, a fluorescence donor can pass its energy to an acceptor group by a radiationless fluorescence resonance energy transfer (FRET) or by collisions. Commonly, both fluorescence donor and a fluorescence acceptor group are appended to probe molecules. In the adjacent probe format, two probes are designed to bind to adjacent segments of the target strand, which brings the labels in close proximity (Fig. 2a) [7,8]. As a result, the fluorescence of the donor dye becomes quenched, whereas acceptor fluorescence is enhanced. The increasingly popular molecular beacons form a hairpin structure with a target unrelated double-stranded stem sequence that holds two reporter groups in close proximity (Fig. 2b) [9]. Annealing of the single-stranded loop segment to the target sequence increases the donor-quencher distance and fluorescence can occur. PCR primers that are equipped with a molecular beacon structure are known as Scorpion^{TM} probes [10,11]. Molecular beacons that are incorporated in the DNA-template strand enable the real-time monitoring of DNA polymerase reaction [12].

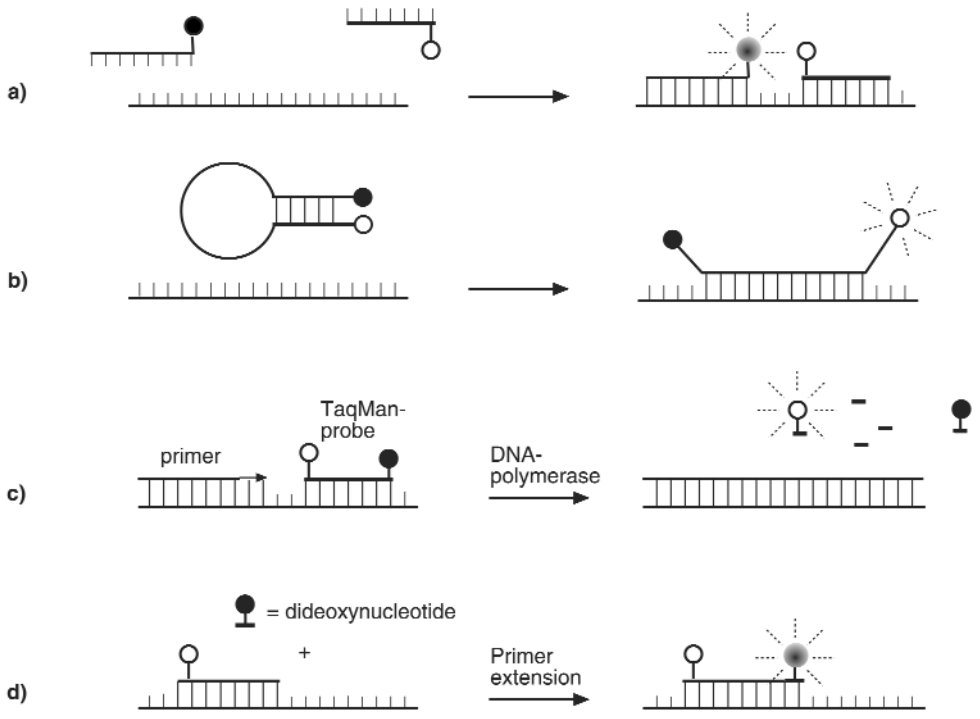

Fig. 2 Homogeneous DNA detection by employing FRET between two labels. Dual label interaction between (a) adjacent probes and (b) in molecular beacons; (c) in TaqMan probes and upon (d) template-directed dye-terminator incorporation.

Dual-labeled oligonucleotide probes known as Taqman probes are amongst the most widely used type of probes in real-time PCR analysis (Fig. 2c) [13]. This is due to the 5'-3' exonuclease activity of *Taq*-polymerase, which provides an effective means of separating the donor from the acceptor fluorophore. PCR-less DNA detection has been enabled by employing an irreversible cleavage of triple-stranded regions, a process known as the Invader assay [14]. The opposite, namely the template-directed coupling of a fluorescently labeled dye-terminator or oligonucleotide segment provided the platform for the development of homogeneous formats of the primer extension [15] (Fig. 2d) and oligonucleotide ligation assays [16], respectively.

The need to use two reporter groups or even two oligonucleotide probes almost inevitably results in increased costs. Hence, there have been efforts to develop one-label detection chemistries, in which an environmentally sensitive fluorophore signals hybridization. The pyrene chromophore was attached to the 5'-end of an oligonucleotide (Fig. 3) [17]. Duplex formation reduced the pyrene emission of **1a** by a factor of 8 due to intercalation. Fontecave and coworkers reported the use of a deazaflavine group in **1b** [18]. Addition of target DNA led to a 20-fold fluorescence decrease. Although the measured fluorescence decays are significant, hybridization-induced fluorescence increases are clearly more desirable. For example, dansyl or pyrenyl groups were introduced at the 2'-position [19,20]. The fluorescence of a pyrenyl oligoribonucleotide (see **2b**) increased by a factor of 16–60 when hybridized with an RNA complement. The hybridization with a DNA strand led, however, to rather poor fluorescence enhancements. The structural basis of this oppositional fluorescence properties is unclear. In RNA duplexes that contained a mismatched base pair in the vicinity of the pyrene group, the fluorescence intensity was dramatically reduced. It is remarkable that the match/mismatch discrimination was accomplished at temperatures below the T_M value.

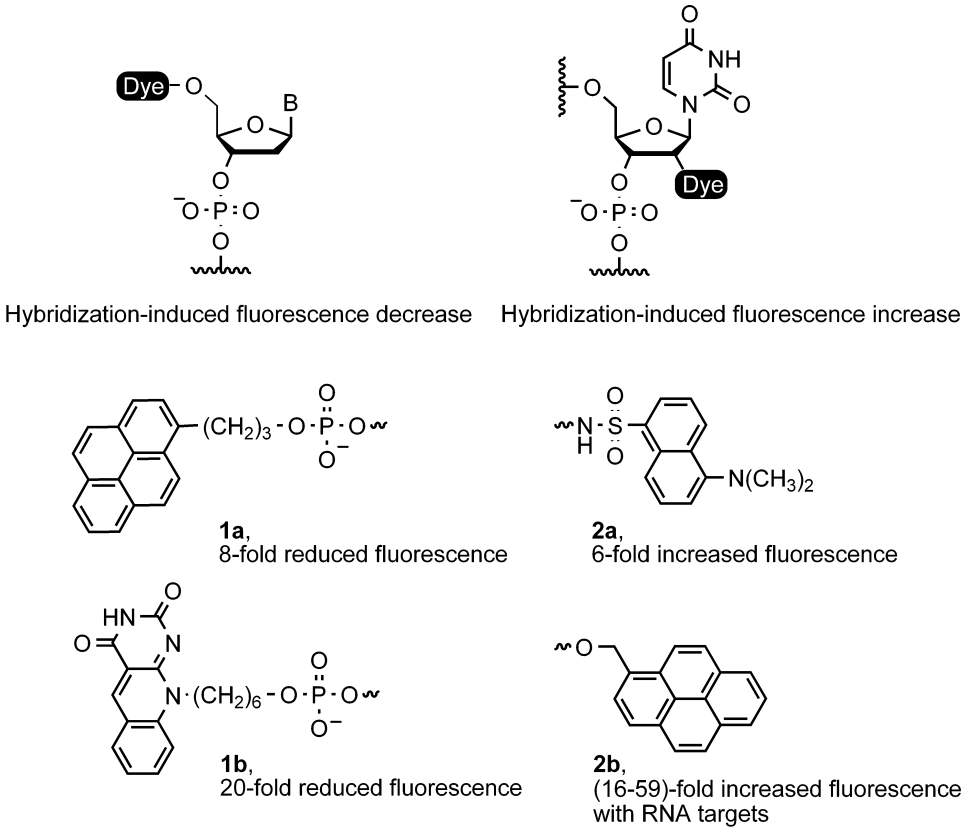

Fig. 3 Environmentally sensitive fluorophores can sense duplex formation.

Intercalator dyes such as ethidium bromide display a particular form of environmentally sensitive fluorescence. Typically, the fluorescence intensity increases upon intercalation. Intercalator dyes were conjugated to probe molecules through a flexible linker, which has to be long enough in order to allow intercalation between base pairs of the formed duplex (Fig. 4). Barton introduced the use of inorganic intercalators such as in **3** [21]. Organic dyes such as oxazole yellow in **4** were applied by Ishiguro and coworkers [22]. Recently, the cyanine dye thiazole orange (TO) was appended to the terminus of the DNA analog PNA (peptide nucleic acid) [23,24]. The fluorescence of mixed sequence duplexes containing PNA-TO conjugates **5** was up to 16-fold higher than single-strand fluorescence. Higher emission intensities were observed when employing oligopyrimidine probes. In one case, a hybridization-induced fluorescence decrease was observed. Similar fluorescence enhancements were determined upon binding to single mismatched DNA as long as measurements were performed at temperatures below the melting temperature of the corresponding PNA-DNA duplex. DNA targets and their respective single base mutants were distinguishable at temperatures that led to dissociation of mismatched complexes.

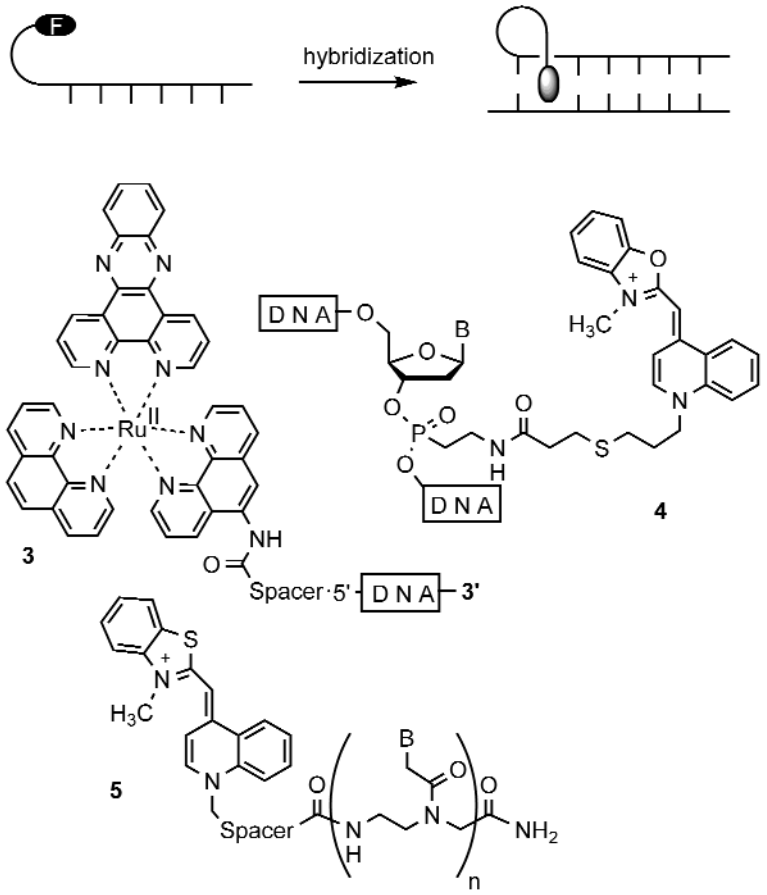

Fig. 4 Homogeneous DNA detection with DNA-intercalator dye conjugates.

An increased selectivity as far as the detection of single base mutations is concerned can be achieved by replacing a nucleobase with a fluorophore (Fig. 5). We envisaged that this *forced intercalation* of fluorophores or fluorescent base surrogates should allow for the detection of structural changes caused by single base mutations or other DNA-modifying events [25]. The fluorescence of the vast majority of base surrogates used to date becomes, however, quenched upon hybridization, resulting in a less desirable negative signal. Intercalator dyes such as ethidium bromide or TO fluoresce upon intercalation between base pairs [26]. However, the replacement of a natural nucleobase by an artificial fluorophore usually results in reduced duplex stabilities. In addition, it would be advantageous if the fluorescent base surrogate proved capable of pairing well to all four natural nucleobases. Such properties have been described for so-called universal bases [27]. For example, 5-nitroindole [28], isocarbostyril [29], and pyrene [30] were reported to nondiscriminately bind within 2–3 °C range of T_M values while destabilizing duplexes by 3–6 °C. The introduction of non-natural bases into DNA is not an easy task owing to the need for a powerful glycosylation chemistry. In contrast, base modifications are easier to implement in the DNA-analogous PNAs. Accordingly, several fluorescent base surrogates such as flavin [31], psoralen [32], and naphthalimide [33] have been placed in the interior of PNA-DNA duplexes. Usually, reduced duplex stabilities were observed. A notable exception is 3,5-diaza-4-oxophenothiazine, which formed stable and fluorescent duplexes [34]. PNA-containing heptafluoronaphthalene showed little base discrimination (1.1 °C), albeit at the cost of a severe reduction of duplex stability (9–12 °C) [35].

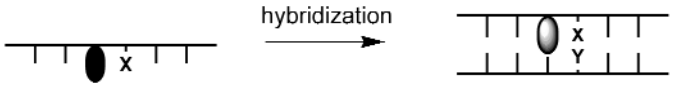

Fig. 5 A fluorophore that serves as fluorescent base surrogate is forced to intercalate adjacent to the expected mutation site. This forced intercalation enables the detection of mismatched base pairs even within a formed duplex.

In the realization of the purpose of replacing a nucleobase, we envisioned that TO should mimic a natural nucleobase as closely as possible. The solution structure of TOTO, a dimeric TO derivative, reveals that the quinoline part is involved in intrastrand stacking interactions, suggesting that TO should be linked to the nucleic acid backbone via the nitrogen of the quinoline ring rather than the benzothiazole [36]. In the context of DNA, the synthesis of monomer unit **6** would be required (Fig. 6). In anticipation of the lability of the *N*-glycosidic bond in **6**, we chose to attach the TO base surrogate to the aminoethylglycine scaffold of the DNA-analogous PNA (see **7**), which provides higher chemical and biological stability.

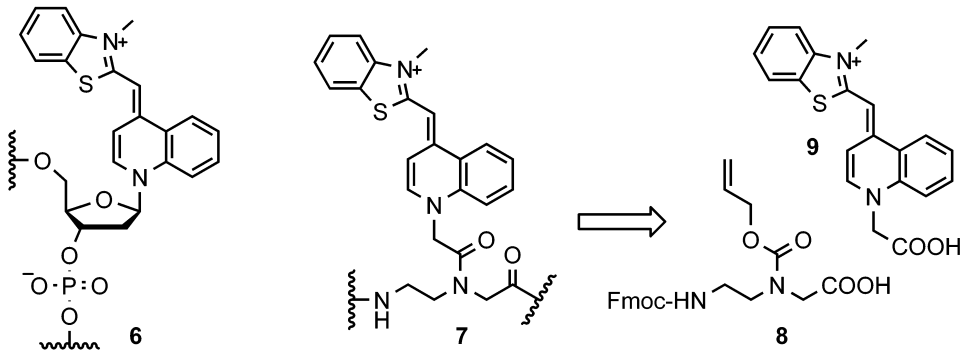

Fig. 6 TO as base surrogate in DNA (**6**) and PNA (**7**). The orthogonally protected aminoethylglycine building block **8** enabled the coupling of carboxymethyl TO **9**.

Instead of preparing a preformed monomer building block, it was preferred to develop divergent access, which in principle would allow the attachment of any carboxyl group containing fluorophore. As the central building block, an orthogonally protected backbone module such as the Fmoc/Aloc-protected aminoethylglycine **8** was incorporated during the Fmoc-based PNA solid-phase synthesis. After completion of the PNA assembly and Pd(0)-mediated removal of the Aloc-group, the full-length PNA resin was allowed to react with TO derivative **9**. The PNA-TO conjugates **10** and **12** were synthesized in the solid phase. RP-HPLC, MALDI-TOF-MS, and UV/Vis confirmed the purity and molecular masses of **10** and **12** and the integrity of the chromophore.

The PNA probes **10** and **12** in which TO was linked via a C2 tether to the quinoline ring at an internal position were hybridized to oligodeoxynucleotide **11** and **13**, respectively (Table 1). The sigmoid behavior of melting curves suggested cooperative base-pairing. PNA-DNA duplexes **10·11** featured TO paired against adenine (**11A**), cytosine (**11C**), guanine (**11G**), and thymine (**11T**). The T_M values averaged to 68 °C within a range of 1 °C. Interestingly, upon formation of natural A-T base pairs in **10A·11T**, a T_M = 69 °C was measurable, which indicates that the TO base surrogate has almost no destabilizing effect. A comparison of the T_M measured for **12·13** and **12C·13** revealed that the replacement of C-G base pair by a TO-G pair reduced duplex stability by only 3 °C. This data allows us to conclude that TO indeed is able to nondiscriminatively pair to all four canonical nucleobases with a "pairing strength" that approaches that of an A-T base pair.

Table 1 T_M data of TO-containing PNA-DNA duplexes.

5'-CGGCT**YZ**TACGGC-3'	Z = A, **11A**; C, **11C**; G, **11G**; T, **11T**				
^{C}Gly-gccgat**X**atgccg$^{N\text{-}Ac}$	X = TO, **10**; A, **10A**				
X-Z[b]	TO-A	TO-C	TO-G	TO-T	A-T
T_M/°C[a]	67	68	68	68	69
5'-CGCTGGAGGTGT-3'	**13**				
^{C}Gly-gcga**X**ctccaca$^{N\text{-}Ac}$	X = TO, **12**; C, **12C**				
X	TO	C			
T_M/°C[a]	66	69			

[a]Measured as denaturation curves at 1 μM concentration in a buffered solution (100 mM NaCl, 10 mM NaH_2PO_4, pH 7).
[b]Y = A.

After having secured the integrity of TO-containing duplexes, we next explored the fluorescence properties of PNA-TO conjugates **10** and **12**. As outlined earlier, TO has low fluorescence in free form, but is rendered highly fluorescent upon intercalation into DNA [26]. Indeed, the addition of complementary DNA to PNA-TO conjugates resulted in enhancements of fluorescence. Figure 7 shows the fluorescence intensifications measured after addition of complementary and single-mismatched DNA as a function of the nucleobase paired against TO. The strongest fluorescence enhancement (11–19-fold) was observed upon formation of perfectly complementary duplexes (blue in Fig. 7). Despite its ability to confer nondiscriminate base-pairing, TO proved able to respond to alterations in its vicinity. The highest emission intensity (19-fold fluorescence enhancement) was determined when TO was paired against thymine. The formation of single-mismatched duplexes led to significantly lower fluorescence intensifications (red in Fig. 7). This data provided a proof-of-principle and suggests that the use of TO as base surrogate allows for a discrimination of matched from single-mismatched DNA. In common DNA-detection chemistries, the detection specificity relies upon the selectivity of probe-target hybridization. The fluorescence of common fluorophores usually is invariant once a probe-target duplex has formed. In these approaches, matched and single-mismatched hybridization cannot be distinguished. In contrast, the TO base surrogate proved sensitive toward structural changes in its envi-

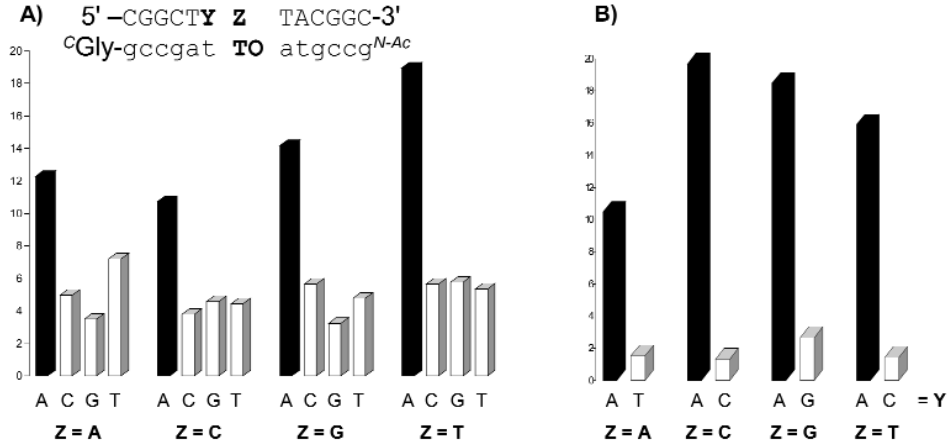

Fig. 7 Fluorescence enhancement after formation of *match* duplexes (filled bars) and *mismatch* duplexes (open bars) at (A) 25 °C and (B) 59 °C. Measurement conditions: 1 μM probes and DNA in buffer as specified in Table 1, excitation: 510 nm, emission: 530 nm.

ronment. It could, hence, be possible to distinguish a DNA target from its single base mutant by avoiding the usual need for stringent hybridization conditions.

In quantitative PCR analysis, DNA detection is performed at temperatures between 55 and 70 °C. Figure 7b shows the fluorescence enhancements measured at 59 °C. At this temperature, the differences between the emission after addition of complementary and the emission after addition of single-mismatched target DNA became more pronounced. Probe fluorescence in the presence of matched DNA was 6–11-fold higher than in the presence of single-mismatched DNA. This enhanced match/mismatch discrimination can be explained by the reduced thermal stability of the mismatched duplex, which is lower by ca. 9 °C when compared with the T_M value of the matched duplex. The fluorescence data suggest that a perfectly complementary target is clearly distinguishable from the single-mismatched strand even at temperatures below the T_M of the mismatched duplex.

PNA probes in which TO was appended to the terminal end (see **5**) have been previously used in real-time quantitative PCR [23,24]. In probe **10**, TO was attached with concomitant replacement of a nucleobase. The fluorescent enhancements measured upon hybridization of our new PNA probe were comparable to those obtained with end-labeled PNA. We therefore expect that the new probes should be applicable in QPCR analysis. The use of TO as base surrogate rendered the emission properties responsive to adjacent base mismatches. In contrast, fluorescence in end-labeled probes usually is invariant once formation of matched or single-mismatched duplexes had occurred. The lower emission of TO base in the presence of adjacent mismatches can be attributed to the locally increased flexibility and less efficient planarization of TO. We expect that probes endowed with the added advantage of being responsive to base mismatches will prove useful in applications where it is difficult to apply stringent hybridization conditions.

FORCED INTERCALATION IN STUDYING DNA–PROTEIN INTERACTIONS

DNA adopts a double-helical structure with the nucleobases buried in the interior of the double helix. For gaining steric access to inner-helical target structures, DNA-modifying enzymes have evolved binding modes that lead to a local disruption of hydrogen-bonding and base-stacking interactions [37–39]. For example, DNA-methyltransferases (DNA-MTases) such as the adenine-specific N^6-DNA-MTase from *Taq*I commence the methyl group transfer by rotating the target base completely out of the helix [40]. As a result of the enzymatic base-flipping process, an unpaired nucleobase remains in the duplex (Fig. 8A). In a minimum model, enzyme binding has to compensate for (1) the dissociation of a Watson–Crick base pair and (2) the formation of an apparent abasic site that interrupts contiguous base-stacking. We envisioned that aromatic base surrogates forced to intercalate opposite to the target base restore the contiguous base stack, which is interrupted upon enzymatic base-flipping, and thus tightens the MTase-substrate complex (Fig. 8B) [41]. In addition, a polycyclic base surrogate destabilizes the inner-helical conformation of the opposing base. The DNA MTase could thus bind to double-stranded

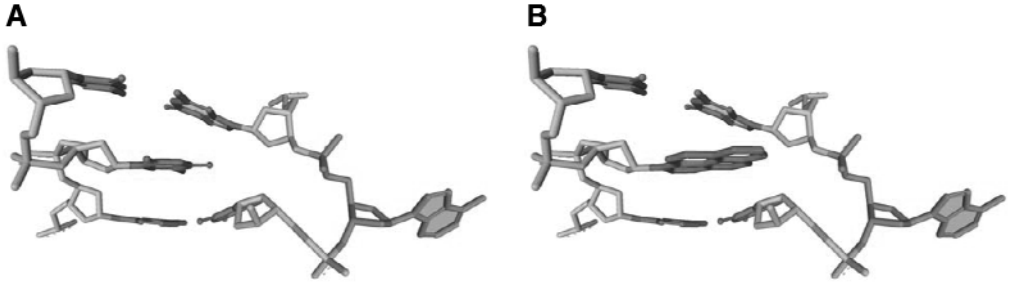

Fig. 8 (A) DNA structure observed in a cocrystal with DNA MTase M.*Taq*I. (B) A modeled replacement, which illustrates that pyrene fits into the cavity left by the flipped adenine and potentially improves interstrand stacking.

DNA containing a preorganized unstacked target base without paying the energetic penalty for disrupting a Watson–Crick base pair and base-stacking interactions.

The incorporation of polycyclic base surrogates into duplex oligonucleotides is achieved by means of *C*-glycosidically modified nucleotide building blocks. The synthesis of the phosphoramidites **18a–e** requires the formation of a *C*-glycosidic bond, which we [42] and others [43] performed according to a protocol from Kool [5] and coworkers who introduced the use of organocadmium reagents (Scheme 1). We sought an alternative *C*-glycosylation method with the aim to replace the toxic cadmium. Organocuprates are known to serve as mild and versatile *C*-nucleophiles in the coupling with primary alkyl, allyl, and benzyl chlorides [44]. Indeed, the reaction of the 2-deoxyribosyl chloride **14** with the Normant reagents **16a–e** proved superior to the analogous reaction with the cadmium organic reagents (Table 2). Removal of the toluoyl groups, regioselective introduction of the trityl group, and final phosphitylation completed the synthesis of the phosphoramidite building blocks **18a–e** [41].

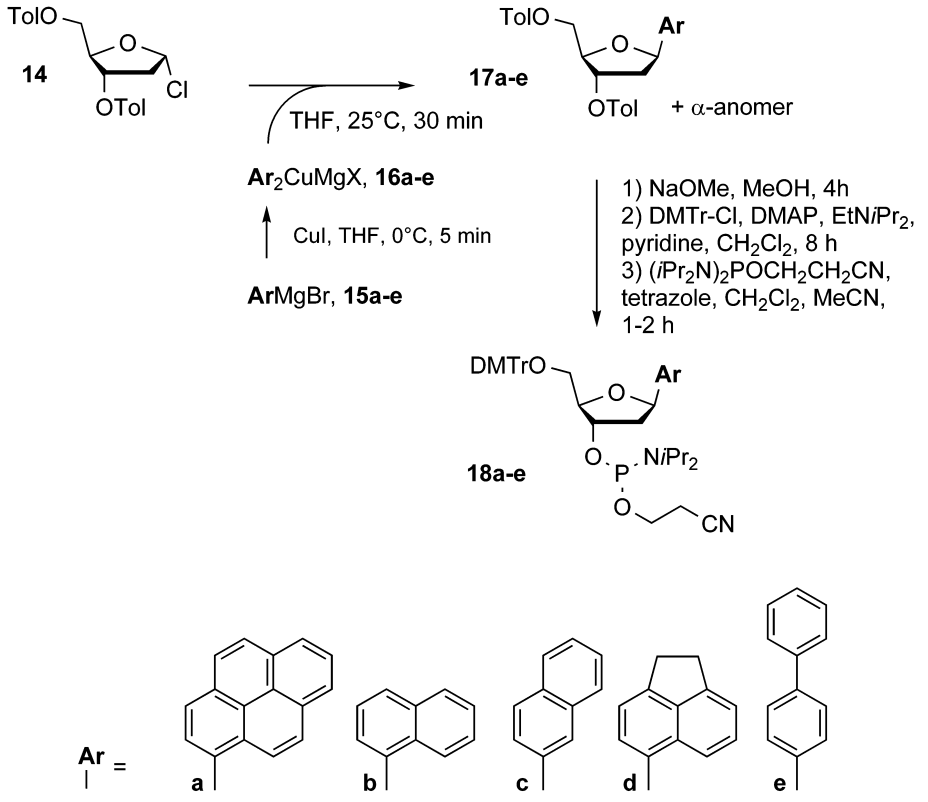

Scheme 1 Synthesis of the *C*-glycoside DNA building blocks **18a–e**.

Table 2 Yields of *C*-glycosylation reactions depicted in Scheme 1[a].

	17a	**17b**	**17c**	**17d**	**17e**
Yield of **17**	74 % (3:1)	81 % (4:1)	74 % (3:1)	47 % (2:1)[b]	75 % (2:1)

[a]The α:β ratio is given in brackets.
[b]Synthesized by using the arylcadmium reagent.

The building blocks **18a–e** were used in automated solid-phase synthesis of oligonucleotides **19a–e** (Table 3) spanning the M.*Taq*I recognition sequence. The modified oligonucleotides **19a–e** were

hybridized with the complementary strand **20A** containing an adenine residue opposite to the base surrogates (Table 3). In all cases, the melting curves showed sigmoid behavior. Substitution of thymine in **19T** by the aromatic base surrogates in **19a–e** led to a decrease of the melting temperature by ΔT_M = –(4.9–8.7) °C.

Table 3 Thermal stability of duplexes and binding affinity to the adenine-specific DNA MTase M.*Taq*I[a].

5'-GCCGC T C G dRibX TGCCG-3'	**20A**, **20b**				
3'-CGGCG A G C dRibY ACGGC-5'	**19T**, **19a-e**				
Y	**X** = adenine, **20A**			**X** = H, **20b**	
	T_M/°C[b]	ΔT_M/K[c]	$K_A/10^9$ M^{-1}	T_M/°C[b]	ΔT_M/K[c]
Thymine, **19T**	65.9	–	0.05 ± 0.02	49.8	–
1-Pyrenyl, **19a**	61.0	–4.9	20 ± 10	63.6	+13.8
4-Biphenyl, **19e**	57.5	–8.4	3.0 ± 1.0	59.0	+9.2
Acenaphthyl, **19d**	59.0	–6.9	2.0 ± 1.0	57.9	+8.1
1-Naphthyl, **19b**	57.2	–8.7	2.0 ± 1.0	56.0	+6.2
2-Naphthyl, **19c**	58.0	–7.9	1.0 ± 0.5	57.8	+8.0

[a]The double-stranded recognition sequence of M.*Taq*I is boxed.
[b]Measured as denaturation curves at 1 μM DNA concentration in a buffered solution (100 mM NaCl, 10 mM NaH_2PO_4, pH 7.0).
[c]ΔT_M values are based on the T_M values of **20A·19T** or **20b·19T**, respectively.

After having secured the integrity of the duplexes **19·20A**, their binding to the M.*Taq*I DNA MTase was investigated in solution. The affinity of M.*Taq*I to the nonfluorescent duplexes **19T·20A** and **19b-e·20A** was determined in a new competitive fluorescence binding assay by using a competitor duplex that contained the fluorescent base analog 2-aminopurine at the target position. This binding assay is not suitable for the duplex **19a·20A** containing the fluorescent pyrenyl residue because the pyrene fluorescence spectrum overlaps with the 2-aminopurine fluorescence spectrum. Therefore, a pyrene fluorescence binding assay was performed which employed a nonfluorescent duplex oligonucleotide as competitor. Native M.T*aq*I binds its unmodified substrate **19T·20A** with a dissociation constant in the nanomolar range. It became apparent that the naphthyl, acenaphthyl, and biphenyl base surrogates enhanced the binding affinity by a factor of 20–60. The about 400-fold enhancement of MTase binding affinity determined for the pyrene containing duplex **19a·20A** was most remarkable. The observed affinity corresponds to a dissociation constant in the picomolar range.

In an attempt to understand the particular role of the pyrene substitution as opposed to the other surrogates, we undertook further experiments with specifically modified DNA complements. Binding of M.*Taq*I to its target DNA leads to the formation of an apparent abasic site, which should destabilize the protein-DNA complex. In general, abasic sites dramatically decrease the duplex stability as exemplified by the substantial reduction of the melting temperature that was observed when the target 2'-deoxyadenosine in **19T·20A** was replaced by the abasic site analog 1,2-dideoxy-D-ribose in **19T·20b** (ΔT_M = –16.1 °C). We explored whether the base surrogates opposite to an abasic site increase the stability of the duplexes **19a–e·20b**. Indeed, each of the abasic site containing duplexes **19a–e·20b** that contained any of the five base surrogates displayed an enhanced thermal stability compared to the thymine-containing abasic site duplex **19T·20b** (Table 3). Most importantly, the thermal stabilities of the abasic site duplexes **19a–e·20b** correlate well with the binding affinities of duplexes **19a–e·20A** to M.*Taq*I (Table 3). The pyrene residue conferred the highest abasic site stabilization and led to the highest binding affinity to M.*Taq*I. Previous experiments with these bulky base surrogates suggested that the biphenyl and not the pyrenyl residue was the most effective base surrogate in disrupting target base-stacking. Thus, we propose that the pyrenyl residue enhances the MTase binding affinity mainly by

compensating the energetic penalty which arises from the enzyme-induced abasic site formation rather than by preorganizing the target base in an unstacked conformation.

CONCLUSION

In conclusion, we have shown that the forced intercalation of aromatic hydrocarbons and heterocycles is a powerful tool in DNA–DNA and DNA–protein interaction studies. TO was demonstrated to confer universal PNA–DNA base-pairing while maintaining duplex stability. The replacement of a central nucleobase with TO afforded a PNA probe that fluoresced upon hybridization. The sensitivity of TO fluorescence to a neighboring base mismatch suggests that it might be possible to distinguish a DNA target from its single base mutant by avoiding the usual need for stringent hybridization conditions. Current work focuses on the detailed analysis of TO fluorescence properties within different sequence contexts.

The data of the DNA-M.*Taq*I binding studies seem to point out that abasic site stabilization is an important criterion for high affinity binding to native DNA MTases. Future work will concern the implementation of this design approach for the development of high-affinity binders to other adenine-specific DNA-MTases from pathogenic bacteria, an endeavor ultimately aiming for the construction of inhibitors of these pharmacologically interesting enzymes.

REFERENCES

1. E. T. Kool. *Acc. Chem. Res.* **35**, 936–943 (2002).
2. D. C. Ward, E. Reich, L. Stryer. *J. Biol. Chem.* **244**, 1228–1237 (1969).
3. M. J. Rist and J. P. Marino. *Curr. Org. Chem.* **6**, 775–793 (2002).
4. E. B. Brauns, M. L. Madaras, R. S. Coleman, C. J. Murphy, M. A. Berg. *J. Am. Chem. Soc.* **121**, 11644–11649 (1999).
5. R. X. F. Ren, N. C. Chaudhuri, P. L. Paris, S. Rumney, E. T. Kool. *J. Am. Chem. Soc.* **118**, 7671–7678 (1996).
6. <www.ncbi.nlm.nih.gov/disease>.
7. M. J. Heller and L. E. Morrison. In *Rapid Detection and Identification of Infectious Agents*, D. T. Kingsbury and S. Falkow (Eds.), pp. 245–256, Academic Press, New York (1985).
8. R. A. Cardullo, S. Agrawal, C. Flores, P. C. Zamecnik, D. E. Wolf. *Proc. Natl. Acad. Sci. USA* **85**, 8790–8794 (1988).
9. S. Tyagi and F. R. Kramer. *Nat. Biotechnol.* **14**, 303–308 (1996).
10. D. Whitcombe, J. Theaker, S. P. Guy, T. Brown, S. Little. *Nat. Biotechnol.* **17**, 804–807 (1999).
11. A. Solinas, L. J. Brown, C. McKeen, J. M. Mellor, J. T. G. Nicol, N. Thelwell, T. Brown. *Nucleic Acids Res.* **29**, E96-U14 (2001).
12. D. Summerer and A. Marx. *Angew. Chem., Int. Ed.* **41**, 3620–3622 (2002).
13. P. M. Holland, R. D. Abramson, R. Watson, D. H. Gelfand. *Proc. Natl. Acad. Sci. USA* **88**, 7276–7280 (1991).
14. R. W. Kwiatkowski, V. Lyamichev, M. de Arruda, B. Neri. *Mol. Diagn.* **4**, 353–364 (1999).
15. X. Chen and P. Y. Kwok. *Nucleic Acids Res.* **25**, 347–353 (1997).
16. V. V. Didenko and P. J. Hornsby. *J. Cell Biol.* **135**, 1369–1376 (1996).
17. J. S. Mann, Y. Shibata, T. Meehan. *Bioconj. Chem.* **3**, 554–558 (1992).
18. C. Dueymes, J. L. Decout, P. Peltie, M. Fontecave. *Angew. Chem. Int. Ed.* **41**, 486–489 (2002).
19. K. Yamana, Y. Ohashi, K. Nunota, H. Nakano. *Tetrahedron* **53**, 4265–4270 (1997).
20. K. Yamana, R. Iwase, S. Furutani, H. Tsuchida, H. Zako, T. Yamaoka, A. Murakami. *Nucleic Acids Res.* **27**, 2387–2392 (1999).
21. Y. Jenkins and J. K. Barton. *J. Am. Chem. Soc.* **114**, 8736–8738 (1992).

22. T. Ishiguro, J. Saitoh, H. Yawata, M. Otsuka, T. Inoue, Y. Sugiura. *Nucleic Acids Res.* **24**, 4992–4997 (1996).
23. N. Svanvik, A. Stahlberg, U. Sehlstedt, R. Sjoback, M. Kubista. *Anal. Biochem* **287**, 179–182 (2000).
24. N. Svanvik, G. Westman, D. Y. Wang, M. Kubista. *Anal. Biochem.* **281**, 26–35 (2000).
25. O. Seitz, F. Bergmann, D. Heindl. *Angew. Chem., Int. Ed.* **38**, 2203–2206 (1999).
26. A. N. Glazer and H. S. Rye. *Nature* **359**, 859–861 (1992).
27. D. Loakes. *Nucleic Acids Res.* **29**, 2437–2447 (2001).
28. D. Loakes and D. M. Brown. *Nucleic Acids Res.* **22**, 4039–4043 (1994).
29. M. Berger, Y. Q. Wu, A. K. Ogawa, D. L. McMinn, P. G. Schultz, F. E. Romesberg. *Nucleic Acids Res.* **28**, 2911–2914 (2000).
30. T. J. Matray and E. T. Kool. *J. Am. Chem. Soc.* **120**, 6191–6192 (1998).
31. H. Ikeda, K. Yoshida, M. Ozeki, I. Saito. *Tetrahedron Lett.* **42**, 2529–2531 (2001).
32. A. Okamoto, K. Tanabe, I. Saito. *Org. Lett.* **3**, 925–927 (2001).
33. H. Ikeda, Y. Nakamura, I. Saito. *Tetrahedron Lett.* **43**, 5525–5528 (2002).
34. L. M. Wilhelmsson, A. Holmen, P. Lincoln, P. E. Nielson, B. Nordén. *J. Am. Chem. Soc.* **123**, 2434–2435 (2001).
35. K. A. Frey and S. A. Woski. *Chem. Commun.* 2206–2207 (2002).
36. H. P. Spielmann, D. E. Wemmer, J. P. Jacobsen. *Biochemistry* **34**, 8542–8553 (1995).
37. R. J. Roberts and X. D. Cheng. *Annu. Rev. Biochem.* **67**, 181–198 (1998).
38. R. J. Roberts. *Cell* **82**, 9–12 (1995).
39. D. P. Hornby and G. C. Ford. *Curr. Opin. Biotechnol.* **9**, 354–358 (1998).
40. K. Goedecke, M. Pignot, R. S. Goody, A. J. Scheidig, E. Weinhold. *Nat. Struct. Biol.* **8**, 121–125 (2001).
41. C. Beuck, I. Singh, A. Bhattacharya, W. Hecker, V. S. Parmar, O. Seitz, E. Weinhold. *Angew. Chem., Int. Ed.* **42**, 3958–3960 (2003).
42. I. Singh, W. Hecker, A. K. Prasad, V. S. Parmar, O. Seitz. *Chem. Commun.* 500–501 (2002).
43. A. K. Ogawa, Y. Q. Wu, M. Berger, P. G. Schultz, F. E. Romesberg. *J. Am. Chem. Soc.* **122**, 8803–8804 (2000).
44. The coupling of glucopyranosyl halides with lithiumdimethyl copper has been demonstrated before: R. Bihovsky, C. Selick, I. Giusti. *J. Org. Chem.* **53**, 4026–4031 (1988).